



HAL
open science

Pantographs bounce modelling for the simulation of railway systems

Saba Amirdehi, Baptiste Trajin, Paul-Etienne Vidal, Johana Vally, Didier Colin, Frédéric Rotella

► **To cite this version:**

Saba Amirdehi, Baptiste Trajin, Paul-Etienne Vidal, Johana Vally, Didier Colin, et al.. Pantographs bounce modelling for the simulation of railway systems. PCIM Europe 2019, Power Electronics - Intelligent Motion - Renewable Energy - Energy Management, May 2019, Nuremberg, Germany. pp.0. hal-02487084

HAL Id: hal-02487084

<https://hal.science/hal-02487084>

Submitted on 21 Feb 2020

HAL is a multi-disciplinary open access archive for the deposit and dissemination of scientific research documents, whether they are published or not. The documents may come from teaching and research institutions in France or abroad, or from public or private research centers.

L'archive ouverte pluridisciplinaire **HAL**, est destinée au dépôt et à la diffusion de documents scientifiques de niveau recherche, publiés ou non, émanant des établissements d'enseignement et de recherche français ou étrangers, des laboratoires publics ou privés.



Open Archive Toulouse Archive Ouverte

OATAO is an open access repository that collects the work of Toulouse researchers and makes it freely available over the web where possible

This is an author's version published in: <http://oatao.univ-toulouse.fr/23875>

To cite this version:

Amirdehi, Saba and Trajin, Baptiste[✉] and Vidal, Paul-Etienne[✉]
and Vally, Johana and Colin, Didier and Rotella, Frédéric[✉]
Pantographs bounce modelling for the simulation of railway systems. (2019) In: PCIM Europe 2019, Power Electronics - Intelligent Motion - Renewable Energy - Energy Management, 5 May 2019 - 7 May 2019 (Nuremberg, Germany).

Any correspondence concerning this service should be sent
to the repository administrator: tech-oatao@listes-diff.inp-toulouse.fr

Pantographs bounce modelling for the simulation of railway systems

Saba AMIRDEHI^{1,2}, Baptiste TRAJIN¹, Paul-Etienne VIDAL¹, Johana VALLY², Didier COLIN², Frédéric ROTELLA¹

¹Laboratoire Génie de Production, LGP, Université de Toulouse, INP-ENIT, Tarbes, France

²Alstom transport, 50 Rue du Dr Guinier, 65600 Séméac, France

Corresponding author: Saba AMIRDEHI, saba.dehghanikiadehi@alstomgroup.com

Abstract

In order to study the effect of pantograph bounce on railway traction chain a global model including the power supply, catenary, transformer and effects of pantograph bounce has to be established. In this paper, pantograph bounce model considering arc model including all significant parameters such as relative airflow, variable disconnection length is presented. Pantograph arc phenomenon is analyzed in the shape of global model of power input of traction. Model is established using bond graph in order to express differential system of equations that can be easily implemented on numerical simulators. Simulation results are compared with experimental results from real train.

1 Introduction

Electrical arcing during pantograph bounce in electrified railway is a common phenomenon. Due to mechanical oscillations of train, pantograph and catenary, irregularity of contact wires and influence of high speed airflow, pantograph and catenary can be disconnected for a period of time [1], [2]. Electrical arc can be modeled through a variable and nonlinear resistance. It influences the available voltage for train traction chain and current of catenary as well [2]. Arcing phenomenon was modeled in detail in previous papers, [3], [4], [5]. Most arc models are presented based on the results from laboratory experiments which are not exactly representative for this phenomenon on complete traction chain [6], [7], [8].

In order to analyze the global influence of pantograph bounce and electrical arcing, it is needed to have a complete model of power supply, catenary and train traction chain.

In this paper, alternating current power chain including pantograph bounce effects is modeled using bond graph. Bond graph allows considering and representing physical phenomenon. Finally state equations of the system are deduced for simulation purposes. In order to validate the proposed model, simulation results are given and compared with real train measurements.

2 Model of the traction chain

2.1 Power part

In order to analyze the effect of electrical arcing during pantograph bounce on the traction chain, it is needed to have an accurate model of whole power supply and traction chain of train. In this approach, power chain from substation to secondary part of transformer is particularly under concern. Electromechanical part and associated power converters of the traction chain are simplified through equivalent voltage sources based on experimental steady state measurements (U_{s1}, U_{s2}). Figure 1 shows the corresponding schematic of the traction chain. At the secondary of the transformer, there are two windings for electromechanical parts and associated converters of traction chain.

While train is moving, there are some variations of Π model of catenary parameters: resistance, capacitance and inductance of catenary depend of distance between the train and the substation [9]. Note that these parameters may also depend on environmental conditions such as temperature of humidity. However, these effects won't be studied in this paper. Only general values of parameters will be indicated and should be adapted. Electrical arc can be modelled as a nonlinear resistance [2]. Therefore, a variable resistance (R_{arc}) represents connection or disconnection of pantograph and catenary

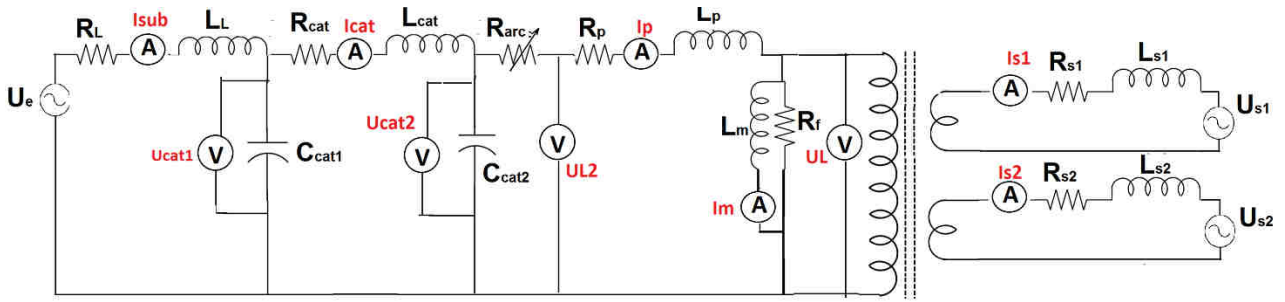


Fig. 1: Power supply, catenary and traction chain including arc resistance.

including arcing phenomenon, in the circuit of figure 1. Table 1 shows all the parameters of circuit in figure 1.

Parameter	Definitions
U_e	Voltage of substation
R_L	Resistance of substation
L_L	Inductance of substation
C_{cat1}, C_{cat2}	Capacitors of catenary
R_{cat}	Resistance of catenary
L_{cat}	Inductance of catenary
R_{arc}	Nonlinear resistance of arc
R_p	Leakage resistance of primary of input train transformer
L_p	Leakage inductance of primary of input train transformer
L_m	Magnetizing inductance of input train transformer
R_f	Parallel magnetizing resistance of input train transformer
R_{s1}, R_{s2}	Resistances of secondary of input train transformer
L_{s1}, L_{s2}	Leakage inductances of secondary of input train transformer
U_{s1}, U_{s2}	Equivalent voltage sources for electromechanical traction chain

Table 1: Parameters of the circuit

In order to have a model of the whole power chain (Figure 1) bond graph method is chosen.

This method illustrates energy transfers in systems by considering power links with two energy variables: generalized effort (voltage) and generalized flow (current) [10]. All physical

phenomena, including integral causality, are modeled by some elements linked by junctions [11]. Figure 2 depicts the bond graph of whole system shown in Figure 1. It can be deduced that the inputs of the system are U_e, U_{s1}, U_{s2} .

Based on bond graph definitions, all the components of the power chain are modelled using elements and junctions as described in table 2:

Parameter	Definitions
$S_e \rightarrow$	Effort source representing voltage source
$\rightarrow R$	Resistance
$\rightarrow I$	Inductance representing electrical inductance
$\rightarrow C$	Capacitance
$\rightarrow TF \rightarrow$	Transformer
$\rightarrow 1 \rightarrow$	1-junction Generalized flows are identical on each power link attached to the junction
$\rightarrow 0 \rightarrow$	0-junction Generalized efforts are identical on each power link attached to the junction

Table 2: Bond graph elements definitions used in figure 3

Bond graph directly allows identifying inputs of the system (generalized effort of effort source) but also state variables (generalized flow of I elements and effort of C elements). Consequently, following junction equations, state equations of the whole system can be directly achieved considering energy variables and causality:

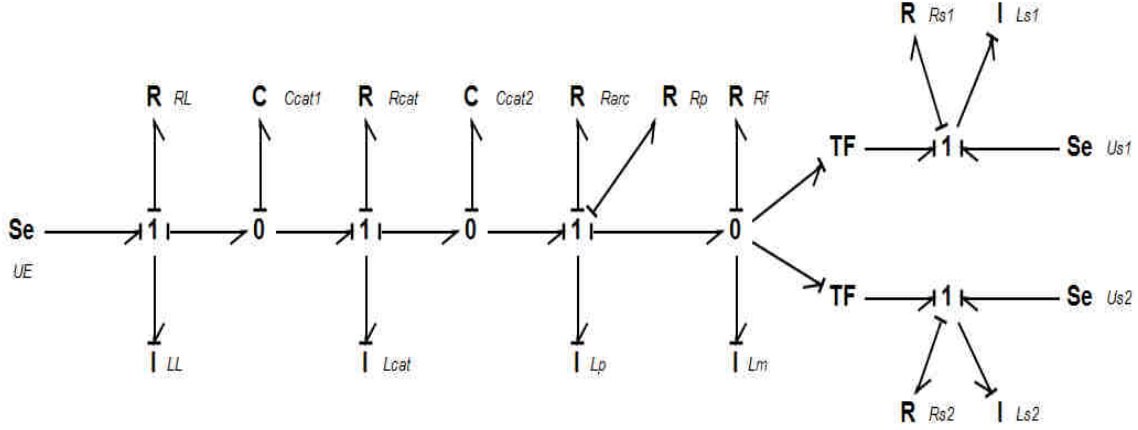


Fig. 2: Bond graph of power supply, catenary and traction chain including R_{arc}

$$\begin{cases}
 \dot{I}_{sub} = \frac{-R_L}{L_L} I_{sub}(t) - \frac{1}{L_L} U_{cat1}(t) + \frac{1}{L_L} U_E(t) \\
 \dot{I}_{cat} = \frac{-R_{cat}}{L_{cat}} I_{cat}(t) + \frac{1}{L_{cat}} U_{cat1}(t) - \frac{1}{L_{cat}} U_{cat2}(t) \\
 \dot{U}_{cat1} = \frac{1}{C_{cat1}} I_{sub}(t) - \frac{1}{C_{cat1}} I_{cat}(t) \\
 \dot{U}_{cat2} = \frac{1}{C_{cat2}} I_{cat}(t) - \frac{1}{C_{cat2}} I_p(t) \\
 \dot{I}_p = \frac{U_{cat2}(t)}{L_p} - \frac{(R_{arc}(t)+R_p)}{L_p} I_p(t) - \frac{U_L(t)}{L_p} \\
 \dot{I}_m(t) = \frac{U_L(t)}{L_m} \\
 \dot{I}_{s1} = \frac{(-R_{s1} I_{s1}(t) + m_1 U_L(t) - U_{s1}(t))}{L_{s1}} \\
 \dot{I}_{s2} = \frac{(-R_{s2} I_{s2}(t) + m_2 U_L(t) - U_{s2}(t))}{L_{s2}} \\
 U_L(t) = R_f (I_p(t) - m_1 I_{s1}(t) - m_2 I_{s2}(t) - I_m)
 \end{cases} \quad (1)$$

where m_1 and m_2 are primary to secondary ratios of transformer.

State equations are useful for simulation purposes due to the possibility to solve the system along time using numerical integration algorithms such as Euler, Heun or Runge-Kutta methods [12, 13].

2.2 Arc Model

Generally, there are four different conditions during pantograph bounce: no arc, arc drawn, arc extinguished and arc approach. Arc drawn happens while distance between pantograph and catenary is sufficiently small and increases. In this case, due to the existence of arc, there is still electrical connection between pantograph and catenary. While this disconnection length

increases until there is no enough energy to maintain the arc, it will be extinguished and the electrical connection of pantograph and catenary will be loosed. Following these steps, pantograph goes back to the catenary. While distance between pantograph and catenary decreases, electrical field increases. So that, arc phenomenon will occur gain. This step is called arc approaching. Note that the maximum arc length in this step is less than the one in the step of arc drawn [4].

Figure 3 shows all the steps of arc drawn, arc extinguished and arc approaching.

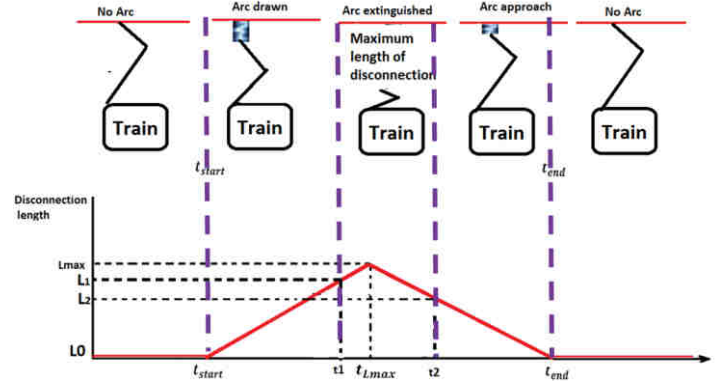


Fig. 3: Pantograph bounces process

During this process, variation of disconnection length along time is considered as a constant [2].

Note that some of these three steps could be neglected due to different case of disconnection on reality. Indeed, arc extinguishing may not appear if the arc length does not exceed its maximum value.

As assumed before, electrical arc is modelled through a nonlinear resistance R_{arc} that depends on the relative position of catenary and pantograph. Obviously, $R_{arc} = 0$ if there is a contact between catenary and pantograph and no arc is created. Moreover, $R_{arc} = \infty$ if there is disconnection between catenary and pantograph without arc phenomenon (arc extinguished).

In this paper, Habedank's equation is used to describe arc phenomenon. Indeed, in case of train study, it allows to take into account effects of airflow speed that can be assumed to be similar to train speed [1]. Moreover, the model describes variations of length between pantograph and catenary denoted in the following $L_{arc}(t)$ [5]. Equation (2) gives arc resistance along time when there is disconnection between catenary and pantograph with arc phenomenon depending on $g_c(t)$ and $g_m(t)$, respectively Cassie and Mayr conductance. Thus, Habedank's model is a series association of Cassie's and Mayr's models. Note that Cassie's model is more adapted for high current values and Mayr's model for arc with low current values [14, 15].

$$R_{arc}(t) = \frac{1}{g_{arc}(t)} = \frac{1}{g_c(t)} + \frac{1}{g_m(t)} \quad (2)$$

Conductance's $g_c(t)$ and $g_m(t)$ are governed by nonlinear differential equations (3) and (4)

$$\frac{dg_c}{dt} = \frac{1}{\tau_2} \left[\frac{I_p(t)^2}{u_c(t)^2 g_c(t)} - g_c(t) \right] \quad (3)$$

where $u_c(t) = CL_{arc}(t)$,

$$\frac{dg_m}{dt} = \frac{1}{\tau_1} \left[\frac{I_p(t)^2}{P_0(t)} - g_m(t) \right] \quad (4)$$

with:

$$\begin{aligned} -P_0(t) &= k g_{arc}(t)^\beta L_{arc}(t)^n \text{ if } v < V_0 \\ -P_0(t) &= a L_{arc}(t) K_1 (v + b) \sqrt{I_{p,rms}(t)} \text{ if } v \geq V_0 \end{aligned}$$

$I_{p,rms}(t)$ is the RMS value over a period of $I_p(t)$

$$\text{with } I_{p,rms}(t) = \sqrt{\frac{1}{T} \cdot \int_{t-T}^t I_p^2(u) du}$$

$\beta, n, \tau_1, \tau_2, v, K_1, k, C$ are respectively constant arc dissipation power, parameter depending on arc phenomenon, time constant, airflow speed, correlation coefficient of dissipated power for arc, pyroelectric coefficient and ratio between $L_{arc}(t)$ and u_c . V_0 is a given airflow speed.

For the parameters k and β , the ranges of their values are $k > 0$ and $0 < \beta < 3$, according to measured data in the pantograph arcing test system developed in [16], [17].

It can be assumed that the minimum values of conductance, i.e. the maximum values of arc resistance occur for $I_p(t)$ close to 0. Thus, voltage spikes appear on primary of transformer for zero crossing current. Considering the elements in the power model, such as inductance and capacitances that change the phase shift of current have to be precisely known at each time in order to have accurate values of voltage. Finally, voltage spikes time location depends on train position regarding substation, catenary parameters and also electromechanical chain that modify phase shift of current on the secondary part of the transformer.

3 Simulation results

In this section, some simulation results will be detailed. First of all, numerical integration algorithm will be detailed. Then, for a given set of parameters, state variables will be studied in case of pantograph approach with arc phenomenon.

3.1 Numerical integration

The solving method chosen for differential equations is Heun method [12]. Let's consider differential equation in (5). From a time instant j , an approximation of state X at time instant $j+1$ is given by (6) with dt the time step between the two time instants.

$$\dot{X} = f(X, U) \quad (5)$$

where X is the vector of state variables and U the vector of inputs.

$$\begin{cases} k_1 = dt \cdot f(X_j, U_j), \\ k_2 = dt \cdot f(X_j + k_1, U_{j+1}) \\ X_{j+1} = X_j + 0.5 * (k_1 + k_2) \end{cases} \quad (6)$$

3.2 State variables

Based on the explanations in section 3.1, the whole circuit of figure 1 is simulated using Heun method. Table 3 shows the value of parameters of circuit that are used in simulation.

Parameter	Values	Parameter	Values
U_E	15 kV	L_p	3.16 mH
R_L	0.14 Ω	L_m	2.5 H
L_L	3.16 mH	R_f	1 k Ω
C_{cat1}, C_{cat2}	0.081 μ F	R_{s1}, R_{s2}	0.32 Ω
R_{cat}	2.95 Ω	L_{s1}, L_{s2}	91.6 mH
L_{cat}	1 mH	U_{s1}	920 V
R_p	0.14 Ω	U_{s2}	920 V

Table 3: Values of circuit parameters used in simulation

Figure 4 shows some of the state variable signals that were obtained by simulation. Arc parameters values were extracted from [2].

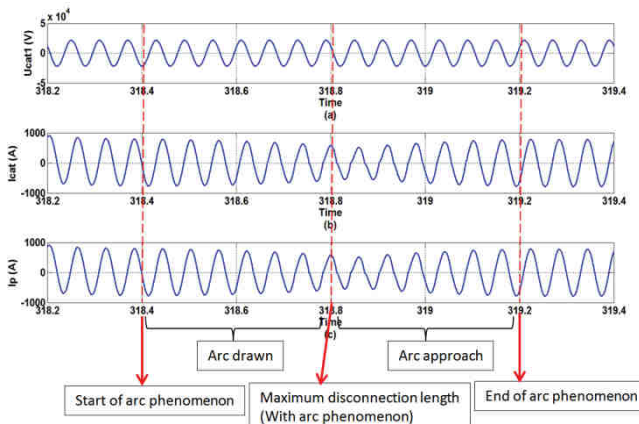


Fig. 4: Simulation result of state variable: a) Catenary voltage, b) Current of catenary, c) Primary current of transformer.

It can be observed that there is an amplitude decrease of the current signals (Catenary and primary of transformer) due to the arc phenomenon. There are no changes in the catenary voltage. Indeed, catenary capacitor may be seen as a voltage source, thus its voltage amplitude may not change during arc. However, as global resistance of the system increases due to arc phenomenon, at constant voltage, catenary and transformer currents may decrease. Some effects also appear on the derivative of currents.

4 Experimental validation

In order to be the most accurate as possible, simulations are performed with similar conditions to tests on train. The detachment of pantograph and catenary was done very fast and no arc was created. Then pantograph is reattached to catenary slowly and the arc phenomenon can be observed. Therefore, all the steps of disconnection between pantograph and catenary are neglected except arc approach. In the step of

simulation, disconnection length is reducing linearly as a function of time.

During the test, substation voltage is 15 kV (RMS) and frequency of 16,2/3 Hz. Train speed is 100 km/h. Therefore, we have $v > V_0$.

Based on the investigation of [2], equation of $L_{arc}(t)$ for simulation part will be as below:

$$L_{arc}(t) = -\frac{L_{max}}{\Delta t}(t - t_2) + L_{max} \quad (7)$$

where:

- $L_{max}=5cm$ the maximum distance between pantograph and catenary,
- $\Delta t=0.5s$ the approach duration,
- $t_2 = 318.05s$ is the start time of pantograph approach.

For the parameters of equation (3), based on the investigation [13], the arc waveform is close to experimental results with $a=0.81$, $b=10$, $K_1=2$, $\tau_1 = \tau_2=0.1$ ms and $C=15$.

All the arc parameters are identified by internal software based on experimental results. Due to the confidential aspects, it is not possible to go in detail about method of identification.

Figure 5 shows the comparison between the train result and simulation result based on the equations (1) and (2).

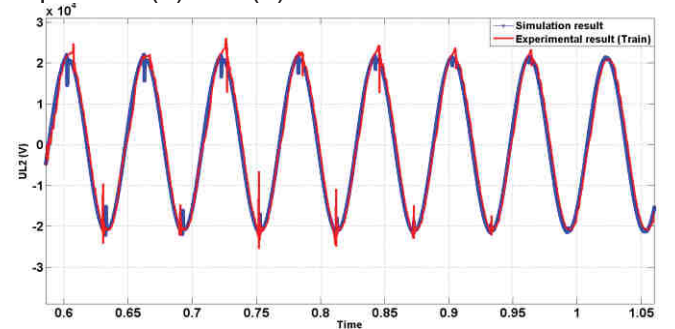


Fig. 5: Primary voltage of transformer on train and simulation in presence of arc phenomenon

It can be seen that effects of arc phenomenon on primary voltage of transformer in simulation is representative of real measurements on train. As explained in section 2, there are two voltage spikes per period due to the zero crossing point of current. Zero crossing point of current are perfectly predicted thanks to modeling of the whole power chain. Due to measurements parameters such as sample time, the comparison of spikes high frequency oscillations are difficult. However, this is balanced by the fact that the worst effect of arcing lies in the values of spikes that can induce overvoltage and then damages in the traction chain.

5 Conclusion and future work

In this paper, pantograph bounce with arc phenomenon was modeled inside a complex power traction chain using bond graph. This model is achieved to lead to state equations that can be easily simulated. The major effects of pantograph bounce are on the input of traction chain: primary voltage and current of transformer. Comparison between real measurements and simulation results shows that presented model is sufficiently accurate to predict the behavior of the whole system during pantograph bounce phenomenon.

In future work, arc behavior regarding parameters of the power chain such as inductance and resistance of catenary and primary of transformer will be studied. A sensitivity analysis will be performed to clearly understand the effect of train distance and speed regarding substation.

6 Acknowledge

This research was supported partially by national association research technology (ANRT).

7 References

- [1] U. Habedank, "On the mathematical-description of arc behavior in the vicinity of current zero," *Etz. Archiv*, vol. 10, no. 11, pp. 339 - 343, 1988.
- [2] Z. Hongyi, L. Zhigang, C. Ye, H. Ke. "Extended black-box model of pantograph arcing considering varying pantograph detachment distance," 2017 IEEE Transportation Electrification Conference and Expo, Asia-Pacific (ITEC Asia-Pacific).
- [3] T. Hiroshi, "Development of a new pantograph contact strip for ultrahigh-speed operations," *Railway Technology Avalanche*, vol. 8, no. 1, pp. 83-85, 2006.
- [4] W. G. Wang, G. N. Wu, G. Q. Gao, B. Wang, Y. Cui, D. L. Liu, "The pantograph-catenary arc test system for high-speed railways," *Journal of the China Railway Society*, vol. 34, no. 4, pp. 22 - 27, Oct. 2012.
- [5] M. T. Cassie, D. B. Fang, "An Improved arc model before current zero based on the combined Mayr and Cassie arc models," *IEEE Trans. on Power Del.*, vol. 20, no. 1, pp. 138 - 142, July 2005.
- [6] W. Wei, J. Wu, G. Gao, Z. Gu, X. Liu, G. Zhu, G. Wu, "Study on Pantograph Arcing in a Laboratory Simulation System by High-Speed Photography", *IEEE Trans. on Plasma Science*, vol. 44, no. 10, pp. 2438 – 2445, 2016.
- [7] T. Li, G. Wu, L. Zhou, G. Gao, W. Wang, B. Wang, D. Liu, D. Li, "Pantograph Arcing's Impact on Locomotive Equipments," 2011 IEEE 57th Holm Conference on Electrical Contacts (Holm), pp. 1 - 5, 2011.
- [8] S. Midya, D. Bormann, T. Schutte, R. Thottappillil, "DC Component rom Pantograph Arcing in AC Traction System - Influencing Parameters, Impact, and Mitigation Techniques," *IEEE Trans. on Electromagnetic Compatibility*, vol. 53, pp. 18-27, 2011.
- [9] J. J Grainger, W. D. Stevenson, "Power systems analysis", McGraw-Hill, 1994.
- [10] G. Gandanegara, X. Roboam, B. Sareni, G. Dauphin-Tanguy, "Modeling and Multi-time Scale Analysis of Railway Traction Systems Using Bond Graphs," *Proceedings of International Conference on Bond Graph Modeling and Simulation*, 2001.
- [11] D.C. Karnopp, R. Rosenberg, A.S. Perelson, "System dynamics: a unified approach," *IEEE Transactions on Systems, Man and Cybernetics*, pp. 724-724, 1976.
- [12] E.Süli, D.Mayers, "An Introduction to Numerical Analysis", Cambridge University Press, 2003.
- [13] W. H. Press, S. A. Teukolsky, W. T. Vetterling, B. P. Flannery, "Numerical Recipes in C, The art of scientific computing", Cambridge University Press, 1992.
- [14] L. Yuan, L. Sun, H. Wu, "Simulation of Fault Arc Using Conventional Arc Models", *Energy and Power Engineering*, vol. 5, pp. 833-837, 2013.
- [15] K. J. Tseng, Y. Wang, D. M. Vilathgamuwa, "An Experimentally Verified Hybrid Cassie-Mayr Electric Arc Model for Power Electronics Simulations". *IEEE Trans. Power Electronics*, vol.12, No.3, pp. 429-436, 1997.
- [16] Y. Wang, "An Extended Habedank's Equation-Based EMTP Model of Pantograph Arcing Considering Pantograph-Catenary Interactions and Train Speeds." *IEEE Trans. on Power Del.*, vol. 31, pp. 1186-1194, June 2016.
- [17] G. Q. Gao, "Study on the mechanism and suppression method of transient overvoltage in the state of fast train," Chengdu: School of Electrical Engineering, Southwest Jiaotong University, 2011